JOURNAL OF SOLID STATE CHEMISTRY 28, 345–361 (1979)

Studies of Layered Uranium(VI) Compounds. I. High Proton Conductivity in Polycrystalline Hydrogen Uranyl Phosphate Tetrahydrate

ARTHUR T. HOWE AND MARK G. SHILTON

Department of Inorganic and Structural Chemistry, University of Leeds, Leeds LS2 9JT, England

Received May 23, 1978; in revised form August 24, 1978.

We have found that hydrogen uranyl phosphate tetrahydrate $HUO_2PO_4 \cdot 4H_2O$ has a high proton conductivity. The ac conductivity was 0.4 $ohm^{-1}\ m^{-1}$ at 290°K measured parallel to the faces of sintered disks of the compound. The activation energy was found to be 31 ± 3 kJ $mole^{-1}$. The values of conductivity were between 3 and 10 times lower when measured perpendicular to the disk faces due to preferred orientation of the plate-like crystals. Both the powder and sintered disks are stable in air and insoluble in phosphoric acid solution of pH 2.5. Experiments are described which enable possible grain boundary contributions to the conductivity to be determined in such hydrates. The extrinsic grain boundary contribution to the conductivity was found to be small from experiments in which the pH in a solution cell was varied. The abnormally high bulk H^+ conductivity thus inferred is attributed primarily to the high concentration of H^+, which exists as H_3O^+ in the interlamellar hydrogen-bonded network. A Grotthus-type mechanism of conduction is proposed which involves intermolecular transfer steps (hopping) and intramolecular transfer steps, in comparable numbers, the former facilitated by the high concentration of H_3O^+ ions in the structure, and the latter most likely facilitated by the high concentration of H-bond vacancies.

Introduction

Metal hydrides are well known for their high hydrogen-ion conductivity. In contrast, up until recently, nonmetallic proton conductors exhibited much lower room-temperature proton conductivities, from approximately 10^{-3} $ohm^{-1}\ m^{-1}$ for hydrated zirconium hydrogen phosphate (*1*), down to approximately 10^{-9} $ohm^{-1}\ m^{-1}$ for KH_2PO_4 (*2, 3*). Proton conductivity in many of these compounds is the topic of several reviews (*4, 5*). However, despite these low conductivities, evidence of high mobilities suggested that high conductivities may be attainable.

Since some early reports indicated that the mobility of protons in ice was unusually high (*5, 6*) and possibly band-type (*7*), and comparable to that found in the metal hydrides, much research has been directed toward increasing the number of charge carriers while retaining a high mobility. The conductivity of doped ice is still, however, comparatively low, and other compounds which have ice-like structures, such as KH_2PO_4, have been studied, again with only limited success (*3*).

Another line of approach, which we, together with other investigators, have adopted, is to study solids in which the fast proton conductivity found in aqueous acid solutions may to some extent be reproduced in the solid by virtue of the presence of rapidly rotating water molecules and free

0022-4596/79/060345-17$02.00/0

hydrogen ions. Just recently two structures which not only have networks of mobile water molecules, but also free excess H^+, have been reported to possess extremely fast H^+ conductivity. Nakamura *et al.* reported, in a patent (*8*), that a range of heteropolymolybdates and heteropolytungstates showed high proton conductivities. For example $H_3PMo_{12}O_{40}\cdot 30H_2O$ and $H_3PW_{12}O_{40}\cdot 29H_2O$, exhibited conductivities in the region of 2 $ohm^{-1}\ m^{-1}$ at 295°K. We have found that acidic hydrates of layered uranyl compounds also possess comparable proton conductivities (*9*). In particular, the compound $HUO_2PO_4\cdot 4H_2O$ (HUP) has a proton conductivity of 0.4 $ohm^{-1}\ m^{-1}$ at 290°K, as reported by us in a preliminary note (*10*). The analogous arsenate also has a similar conductivity (*9*). In this class of compound an acid solution may be considered to be interspaced between the negatively charged uranyl phosphate layers, thereby accounting for the high proton conductivity. It seems likely that a similar explanation may also account for the high conductivity of the heteropolyacids, since the sphere-like heteropolyanions are surrounded by the water molecules, among which the acidic protons may move. Other layer structures have been investigated such as $(Cu(HCO_2)\cdot 4H_2O$ (*11*), for which a conductivity of only approximately 10^{-5} $ohm^{-1}\ m^{-1}$ was found at 273°K.

From a technological point of view, this strategy has been extended to the field of organic ion exchange membranes, in which the negative framework is the organic matrix. Moist Nafion,[1] for example, is a good proton conductor when in the H^+ form. Moreover the conductivity can be enhanced by uptake from an acid solution of H^+ and an equivalent quantity of anions (*12*), which then behave as an immobilized electrolyte within the pores of the material. Zirconium hydrogen phosphate also appears to have some capacity for immobilizing electrolyte (*1*). Many other porous materials show a similar behavior, and the distinction between pore or grain boundary conduction due to absorbed acid and true bulk conduction within the crystalline particles of a pressed disk is often difficult to establish experimentally. We shall describe a method of making such a distinction later in the paper.

In this paper we wish to describe conductivity studies on HUP. The material can be pressed into sintered transparent disks which are stable in air and insoluble in solution. The compound thus provides a much-needed rapid H^+ conducting solid electrolyte for a whole range of electrochemical applications. For instance, proton conduction in electronic conductors could be studied using such a solid electrolyte placed between metal hydride electrodes (*13*). Such a solid electrolyte also has novel applications in the field of solid-state batteries (*13*), electrochromic cells, and possibly fuel cells, electrolysis cells, and other devices (*9*). The disks are stable in a higher pH range than the very acidic, corrosive, and soluble heteropolyacids and are likely to have advantages of ion selectivity and a higher impermeability to gases than the organic polymers.

HUP belongs to a large class of compounds (*14*) of general formula $M^{m+}_{1/m}UO_2XO_4\cdot nH_2O$, where M can be most mono-, di-, or some trivalent cations, and X can be P, As, or often V. Weigel and Hoffmann have provided an extensive review (*15*). Layers of UO_2^{2+} and XO_4^{3-} groups coordinated in a waffle-like square net array are common to all of the compounds. In the phosphate minerals autunite ($M = Ca^{2+}$) and torbernite ($M = Cu^{2+}$) a mirror plane exists between the layers. On the other hand, the layers are displaced sideways relative to each other in *meta*-autunite, *meta*-torbernite, and also in the H^+ and alkali-metal phosphates and arsenates. The interlamellae spaces are

[1] Nafion is the registered trademark of Du Pont for its perfluorocarbon sulfonic acid polymer.

occupied by the water molecules and the exchangeable cations.

The many investigations of HUP (*15–29*) have been mainly performed on synthetic samples: the mineral form exists but is extremely rare (*23, 24*). Three crystalline modifications of HUP have been reported by Moroz (*25*), and a rationalization of the various previously reported cell parameters was made on this basis. It is now evident that the tetragonal polymorph (type I according to Moroz *et al.*) with space group $P4/ncc$, has been studied by Weigel and Hoffmann (*15*), ourselves, Moroz *et al.* (*25*) and Morosin (*29*), who reported a single-crystal X-ray study. The tetragonal polymorph with probable space group $P4/nmm$ (type III), has been studied by Ross (*18*), Williams (*24*), and Moroz *et al.*, while the monoclinic form (type II) has been studied by Moroz *et al.* and possibly also by Walenta (*23*) and Weiss *et al.* (*19*). Unfortunately many reports have not included the cell dimensions to enable polymorph identification (*17, 20–22, 26–28*), although this may not be a problem up to date since, on the basis of the available optical and chemical properties, the polymorphs appear to be indistinguishable (*25*). A single-crystal study of a mixed potassium–hydrogen uranyl arsenate failed to locate the potassium ions (*30*). Comparison of the above single-crystal results with those obtained for copper *meta*-torbernite (*31*) shows that the structural arrangement of both the uranyl phosphate layers and the hydrogen-bonded water network is essentially unchanged by cation replacement.

Most studies report the composition of the maximum hydrate as $HUO_2PO_4 \cdot 4H_2O$ (*15, 19, 20, 26*), although some spread in the water content may be possible (*25*). Atmospheric water vapor pressures exceed the room-temperature equilibrium water vapor pressure of a few millimeters of mercury (*26*), and the compound is stable in air up to about 310°K before undergoing stepwise dehydration to forms with approximately 2, 1.5, and possibly 0.5 waters of crystallization, to eventually produce HUO_2PO_4 at about 430°K (*15, 28*). Heating under reduced water vapor pressure produces only a monohydrate intermediate (*19, 26*). Infrared studies show the presence of H_3O^+ only in the tetrahydrate (*25, 27*). We have reported pulsed NMR studies of HUP and the analogous arsenate and have proposed diffusion and conduction mechanisms which account for both the NMR and conductivity results (*32*). HUP is stable in phosphoric acid solutions of several molar strength up to pH 2.5 (*17*), where the solubility is only 10^{-3} *M* (*22*). Ion exchange, to form the more stable and more insoluble alkali–metal analogs, appears to occur via a dissolution and reprecipitation mechanism (*20, 21*). Previous to our work, studies of ionic conduction of the exchangeable ions in any of the compounds had not been reported.

Results

Preparation and Characterization of HUP

HUP was precipitated from solutions at room temperature containing equimolar proportions of uranyl nitrate (AR) and phosphoric acid (AR), made up with distilled water. We found that a solution of 2.3 *M* phosphoric acid added to a concentrated uranyl nitrate solution slowly produced a finely crystalline product whose particle size was particularly suitable for fabricating into sintered compacts. Although greater yields and higher precipitation rates were obtained using more dilute solutions, the precipitate had poorer fabrication properties.

Disk-shaped compacts of HUP were pressed in a device similar to those used in pressing KBr disks (*9*). Dry powder could be pressed into robust disks which were usually opaque. Disks which were transparent could, however, be pressed, if the starting material was a freshly prepared paste of HUP, which had not been separated from its equilibrium

precipitation solution. Upon maintaining a pressure of 2 tons cm^{-2} (20 MN m^{-2}) the disks gradually became transparent over a period of about 2 days. Much higher pressures applied for short periods of time did not produce transparent disks, showing that densification was occurring via a sintering mechanism. This is thought to involve a dissolution–reprecipitation mechanism in which points of contact transfer to less strained regions. Transparent disks had a measured density of 99.4 ± 1% of the theoretical value for the type I phase (3.43 g cm^{-3}).

The composition of HUP was determined by chemical analysis for uranyl and phosphate, by titration for H^+, and by TGA for water. The results for the air-dried powder were consistent with the formula $HUO_2PO_4 \cdot 4H_2O$. TGA results for pressed disks also showed four waters of crystallization. X-Ray data were obtained on a Philips powder diffractometer using Cu or, for more accurate work, Cr radiation (λ = 229.1 pm).

The preparations consistently produced HUP of type I. The diffractogram of the powder is shown in Fig. 1a, and the low-to-medium-angle lines are indexed. Unit cell parameters of $a = 698 \pm 2$ and $c = 1743 \pm 3$ pm were calculated using the parameters of the intense peaks obtained using Cr radiation. The values agree well with those reported previously (*15, 25*) (for the type I form) and agree reasonably well with the single-crystal study; $a = 699.5(2)$ and $c = 1749.1(4)$ pm (*29*). The diffractograms of disks left in air, and left in phosphoric acid of pH 2.4 for 1 week, showed no change. Figure 1b shows the diffractogram of a disk taken with the X-rays incident on the flat surface of the disk. The relative intensification of the 00*n* peaks indicates substantial flat alignment of the platelets in the disk. We did observe the presence of several additional peaks very close to the (002) peak after repeated scanning in the diffractometer, and also in material precipitated from warm solutions. The peak positions did not correspond to those expected from the type II or type III forms. We now know that these effects are caused by reaction with atmospheric ammonia.

Measurement of Conductivities

In previous studies of hydrates which show a low proton conductivity compared to HUP, the use of single crystals has been imperative in order to eliminate grain boundary and other nonbulk contributions. In such typical materials, an observed conductivity of even 10^{-5} ohm^{-1} m^{-1} is comparable to that found in normal distilled water of pH 5 or 6, and if a pressed pellet were used there would be a large uncertainty as to the possible contribution of water in the grain boundaries or even in cracks or voids. This would be an even more serious problem if the material were an acid hydrate, for which the grain boundaries may be quite acidic. The apparent need for single crystals has undoubtedly hindered development in this area.

However, if the conductivity of the bulk material is much higher than that of the classical proton conductors so as to be in a range comparable to acidic solutions of a concentration considerably above distilled water, then, for insoluble materials, one can utilize a technique which is suitable for pressed pellets. (Single crystals of highly insoluble materials are generally difficult to grow.) We have used the pellet technique for HUP. In order to take account of any extrinsic effects, the conductivity was measured with the disk in contact and equilibrated with solutions of various pH values. If ions external to the bulk crystallites were contributing to the conductivity, the conductivity values would change with pH as the internal ions equilibrated with the external solution. A plot extrapolated to low comparative solution conductivities would give the true intrinsic conductivity. The results of such

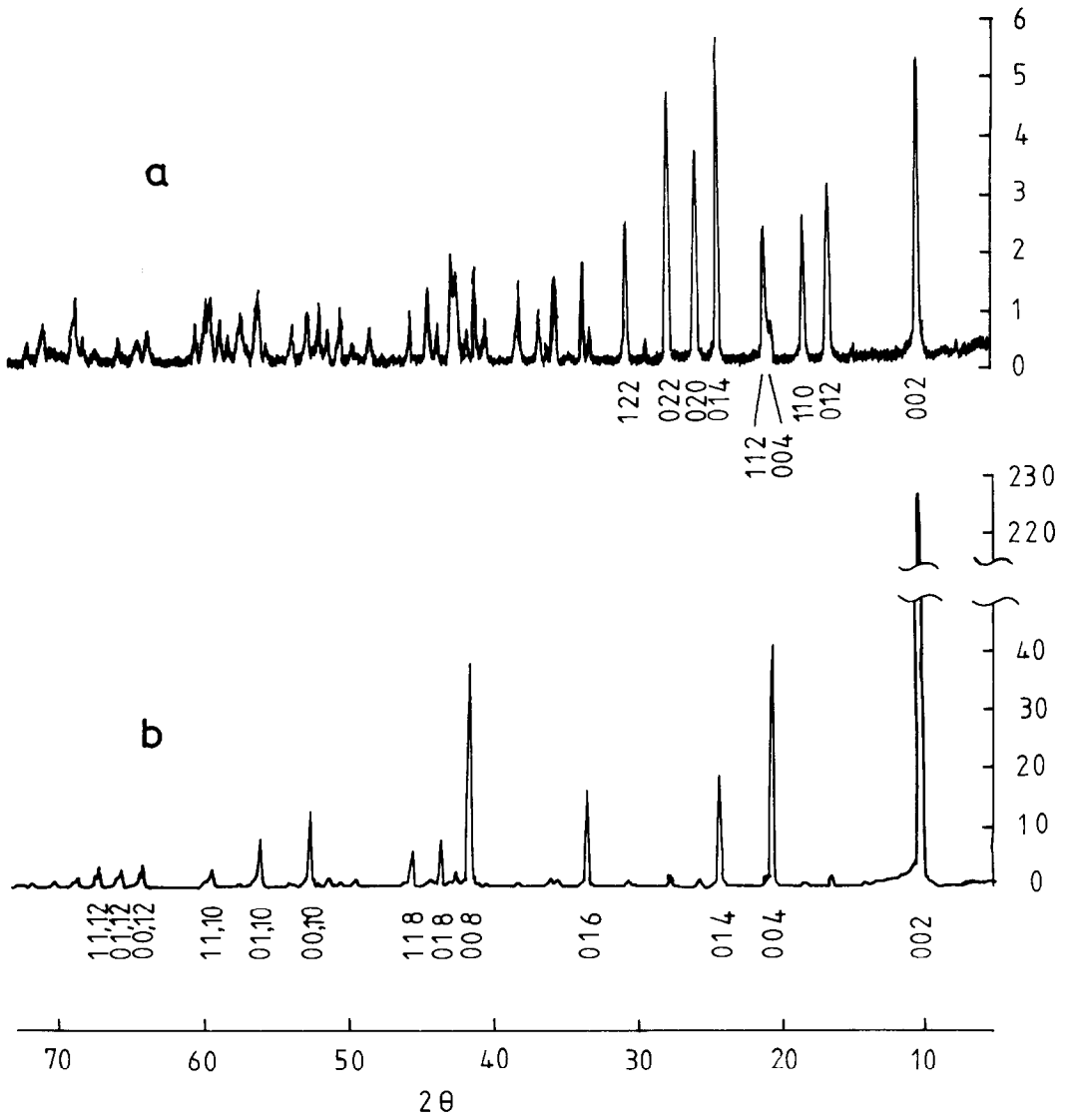

FIG. 1. X-Ray powder diffractometer traces of HUP as (a) air-dried powder, (b) a pressed disk lying flat. using Cu radiation.

experiments using HUP will be described in the following sections.

The above method should also reveal the contribution to the conductivity of gross features such as cracks in the sample or of linked voids between the particles. However, at a density greater than about 95% of the theoretical value any voids present cease to provide a continuous pathway. Penetration of external solution in dense disks such as the HUP disks can therefore only occur via the disordered grain boundary regions. In a layer structure such as HUP, stress in the grain boundary regions is likely to be quite disruptive, to the extent of altering the spacing between the layers and disorienting adjacent layers. At the extreme grain boundary interfaces, fragments of layers may exist, together

with water molecules and charge balancing H^+ ions, which may be more solution-like than bulk-like. The concentration of the charge-balancing H^+ will be fixed by the $(UO_2PO_4)_n^{n-}$ fragments, and will therefore be nonexchangeable. Any conductivity which may arise from such protons will be termed intrinsic grain boundary conduction, as distinct from the contribution, in the same grain boundary regions, of exchangeable ions (an equal number of anions and cations) which will be termed extrinsic grain boundary conduction. The following experiments were designed to reveal any contribution from extrinsic grain boundary effects, and also to determine any possible electrode or interface effects.

Proton Supply from Acidic Solution

The possible effects of extrinsic grain boundary conductivity were investigated by measuring the conductivity of a number of disks as a function of pH of the external solution. The cell configuration was

Pt black | acid soln | HUP | acid soln | Pt black.

The Pt-blacked electrodes had an area of 1 cm^2, which greatly exceeded the area of the HUP disks, so as to reduce any possible polarization effects, which should be considered for such highly conducting disks. Also, in order to minimize any possible surface polarization, an acid solution was interposed between the disks and electrodes to form reversible contacts. A disk was set using araldite into a hole in a glass separator between two well-stirred solutions of equal concentrations of phosphoric acid, thermostated to 307.6°K. The electrodes were set 1 cm back from the disks. Alternating current conductances were measured using a universal Wayne–Kerr bridge (type B221) operating at 1592 Hz, or, for some measurements, operating with an external source and detector over the range 150 Hz to 20 kHz. In addition to the cell conductances, the solution conductances on either side of the partition were measured using a secondary set of Pt-blacked electrodes.

Figure 2 shows the changes in the cell resistances for two disks as a function of solution resistances, as determined by altering the pH of the solutions. For all but the very low pH values, the data show a linear relationship, which has a nonzero intercept. This is indicative of a circuit for which the impedances of the solutions on either side of the disk act in series with a disk impedance which is independent of the pH of the solutions: $Z_{cell} = Z_{soln} + Z_{disk}$. A plot of R_{cell} against R_{soln}, which is proportional to Z_{soln}, will thus give R_{disk} as the intercept.

The upper data in Fig. 2 were obtained from a disk section set such that the conduction direction was parallel to the lie of the platelets comprising the disk. The area was 0.032 cm^2 and the length was 0.40 cm, giving a value of l/A of 12.5 cm^{-1}. The conductivity calculated from the intercept and this value of l/A was 0.83 ± 0.08 $ohm^{-1}\,m^{-1}$. The lower data were obtained for a disk section set such that the conduction direction was perpendicular to the lie of the platelets in the disk. The area was 0.070 cm^2 and the length 0.050 cm, giving an l/A value of 0.715 cm^{-1}.

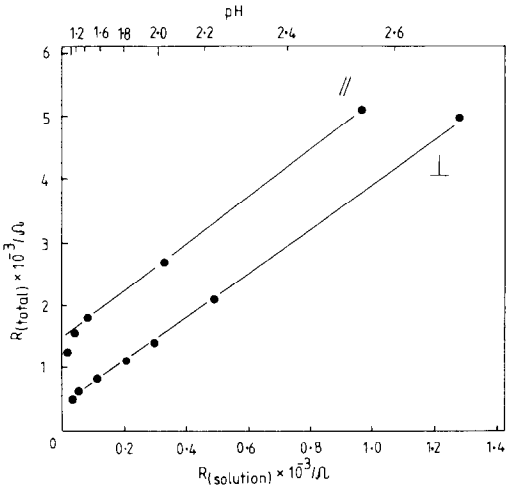

FIG. 2. The total resistance, measured through HUP disks, set parallel and perpendicular, as a function of the surrounding solution resistance, at 307.6°K.

The resulting conductivity calculated from the intercept was 0.19 ± 0.02 ohm^{-1} m^{-1}.

The results show that the conductivities of the disks are independent of the external solution conductivities over the pH range 1.5 to 2.7, and that the observed conductivities are therefore a property of HUP, although this evidence alone does not permit a distinction to be made between true bulk conductivity and intrinsic grain boundary conductivity.

The parallel conductivity of 0.83 ± 0.08 ohm^{-1} m^{-1} at 307.6°K is equivalent to the conductivity of a phosphoric acid solution of pH 2.25 at the same temperature. Now it will be seen from Fig. 2 that at pH values less than 1.5 the cell resistances show a nonlinear decline. This is attributed to uptake of phosphoric acid by the grain boundaries to an extent which creates highly conducting grain boundaries. An estimate of the effective cross section for extrinsic grain boundary conduction can be obtained if we assume that the concentration of extrinsic phosphoric acid in the grain boundaries equals that of the solution at low pH values. At pH 1.0 for the parallel disk the divergence of the data from the straight-line plot reveals a grain boundary conductance of approximately 10 times greater than the bulk conductivity at this pH value, the effective cross section for extrinsic grain boundary conduction would be 1%. This is not an unreasonable value.

It was found that at pH values less than 1 the quality of the disks deteriorated over a period of days, as evidenced by the disks becoming opaque. This is attributed to grain boundary enlargement due to the more rapid rate of dissolution–reprecipitation at the lower pH values. The low pH values shown in Fig. 2 were recorded several hours after the pH had been changed in order to minimize the effect of deterioration. This was, however, sufficient time to allow diffusion of external ions in or out of the grain boundaries. A rough calculation gave a few minutes for this to occur if the mobility of the slowest-moving ions, the phosphate ions, is taken to be the same as in solution, which may be an overestimate. At pH values between 2 and 2.7 the cell resistances were essentially time independent. One disk was continuously measured over a range of pH values between 1.5 and 2.5 for more than 1 month, and the disk remained transparent and the values were reproducible.

Proton Supply from Palladium Hydride

In a second type of experiment small palladium-blacked electrodes in the form of short wire tips were firmly embedded into the surfaces of the HUP disks, and maintained in position with spring loadings. The disks were mounted in a glass divider and immersed in phosphoric acid solution as before. In this configuration there should be no contribution from the external solution resistance. Figure 3 shows the plot of total resistance versus solution resistance over a range of temperatures for a parallel-mounted disk.

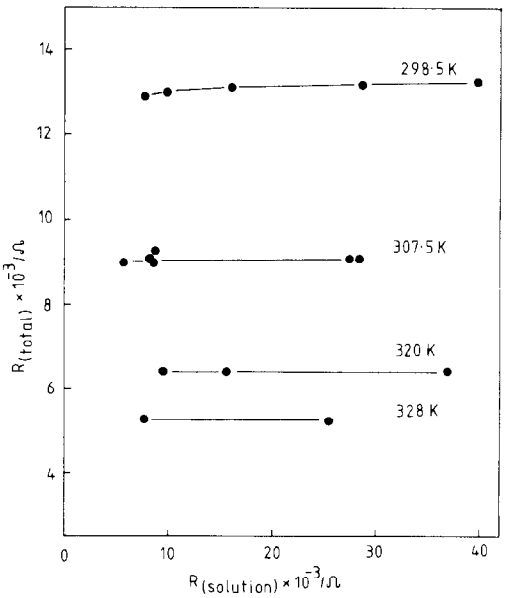

FIG. 3. The resistance of a HUP disk, set parallel, and using palladium hydride proton supply electrodes, as a function of surrounding solution resistance and temperature.

(The solution resistances shown in Figs. 2 and 3 were measured with electrodes of different size and are therefore not comparable.) It can be seen that over most of the pH range the total resistances are indeed constant, with the values representing the intrinsic conductivities of the disks, in confirmation of our earlier conclusion.

It was of interest to extend the measurements up to higher pH values where eventually the increased resistivity of the grain boundaries may block conduction. The pH of the measurements in Fig. 3 ranges from 3.4 to 4.2 for the 307.5°K data. It is apparent that the extrinsic grain boundaries are not blocking over this range. If the grain-boundary ionic concentration equaled that of the external solution, and if we assume a 1% relative grain boundary cross section, we might expect the total grain boundary contribution to equal the intrinsic contribution to the conductivity at pH approximately 4. Evidently pH values higher than 4, which we did not use, are necessary to observe this effect. The results nevertheless imply that the grain boundary relative cross section is indeed not greater than 1%.

Since HUP slowly transforms to the insulating compound $(UO_2)_3(PO_4)_2 \cdot nH_2O$ at pH values greater than about 2.5 (*17*), a coating of this material slowly formed at high pH values on the faces of the disks which were not protected by the electrodes. However, because the electrodes were embedded into the disk surfaces the relative conductivity values were unaffected by the surface reaction over periods of several hours. A few check measurements made at pH 4 the day after the data shown in Fig. 3 were taken showed that, under the same conditions, the resistance had increased by about 10%, undoubtedly due to the slow transformation to uranyl phosphate and possibly to metal-substituted forms of HUP, which may begin to form when the H^+ concentration is low.

One consequence of such reactions is the effect on the resistance of transforming the surface layers back into HUP at lower pH values. This will result in an effective change in l/A due to the additional conduction pathways from the stem of the bar electrodes, through the solution, to the exposed faces of the disks not covered by the electrode. Such a small drop in resistance is evident at the low pH end of the data taken at 298.5°K, where the pH values are less than 3 (the pH rises with increasing temperature).

Whereas in the case of proton supply from solution there was negligible frequency dependence of the ac conductivity, it was found that for the above system there was a frequency dependence of up to 20% between 1592 and 10 000 Hz. The values shown in Fig. 3 were measured at 10 kHz and gave an activation energy for the conductivity of 27 ± 5 kJ mole^{-1} calculated over the temperature range 298.5 to 328°K. The values obtained at 1592 Hz in fact gave the same activation energy, within the rather wide error limits. This indicates that although some polarization is occurring, the activation energy for the partially limiting surface step is not substantially greater than that for disk conductivity, which the value obtained therefore pertains to.

Quantitative Conductivity Values: The Use of Pressed Plate Electrodes

Accurate conductivity values were obtained by pressing against the disk faces palladium-blacked stainless steel cylinders of areas equal to or greater than those of the disks. Two sets of data spanning the temperature range 270 to 373°K are shown in Fig. 4. We shall describe each of these separately. The experimental configuration for the measurements made parallel to the disk flats is shown in Fig. 5. The ground disk of length 0.615 cm and area 0.0242 cm^2, giving an l/A of 25.4 cm^{-1}, was sealed with araldite into a dissected glass tube, to which was then attached a glass partition sheath

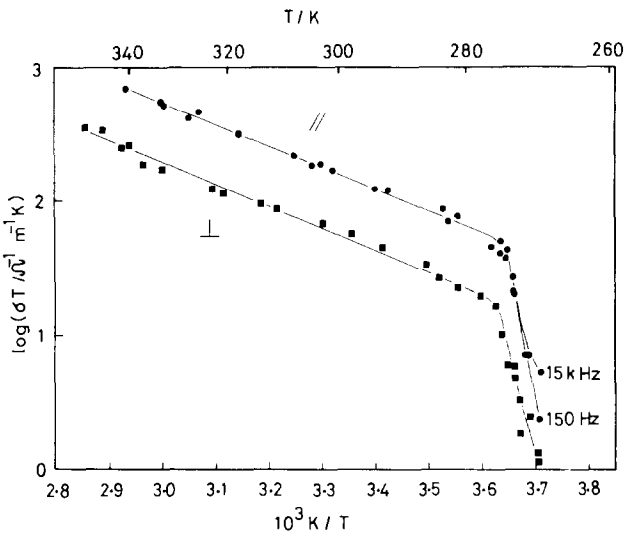

FIG. 4. Conductivity multiplied by temperature of HUP, set parallel and perpendicular, as a function of reciprocal temperature. The frequency dependence above the transition is less than the point size. The data represent values obtained during successive temperature cycling.

as shown. Both sides of the partition were filled with phosphoric acid solution of pH 2.45 which could enter the tube to reach the disk. The palladium-blacked plungers were then inserted and spring loaded onto the disk faces. Positioning pins at top and bottom prevented rotational movement. The outer solution was vigorously stirred, and electrically heated. A proportional controller maintained the temperature to within 0.1°K.

At the electrode–disk junction the high points of the disk surface would be in direct contact with the palladium black. For the remainder of the surface there will be interposed a thin layer of solution. This, together with the contacting palladium hydride, constitutes the electrode system. The thin solution layer will not contribute detectably to the cell resistance, which will therefore represent the disk resistance. The conductivity of the pH 2.45 solution roughly matches that of HUP so that grain boundary effects will be further minimized.

The second set of results, for conductivities perpendicular to the disk flats (Fig. 4), were obtained using a disk pressed hydraulically using palladium-blacked plungers, which subsequently remained stuck to the disk. The assembly was slid into tightly fitting plastic tubing and the measurements were performed in air. It was assumed that there was integral electrode contact to the entire disk area.

As can be seen from Fig. 4, the conductivity is again larger in the parallel direction than in the perpendicular direction (by a factor of about 3). The conductivity in the parallel direction was 0.4 $\text{ohm}^{-1}\,\text{m}^{-1}$ at 290°K. Above 274°K both sets of data showed the same activation energies, obtained from a log σT vs $1/T$ plot, to within experimental error, this being 31 ± 3 kJ mole^{-1}. The plot of log σ vs $1/T$ gives a value of 30 kJ mole^{-1} for the same data, as previously reported (*10*). In this temperature region there was only about a 5% increase in conductivity between 150 Hz and 20 kHz for both sets of data, showing only minimal polarization effects. The conductivities and activation energies should therefore relate to disk and not interfacial properties, which is supported by the agreement between the

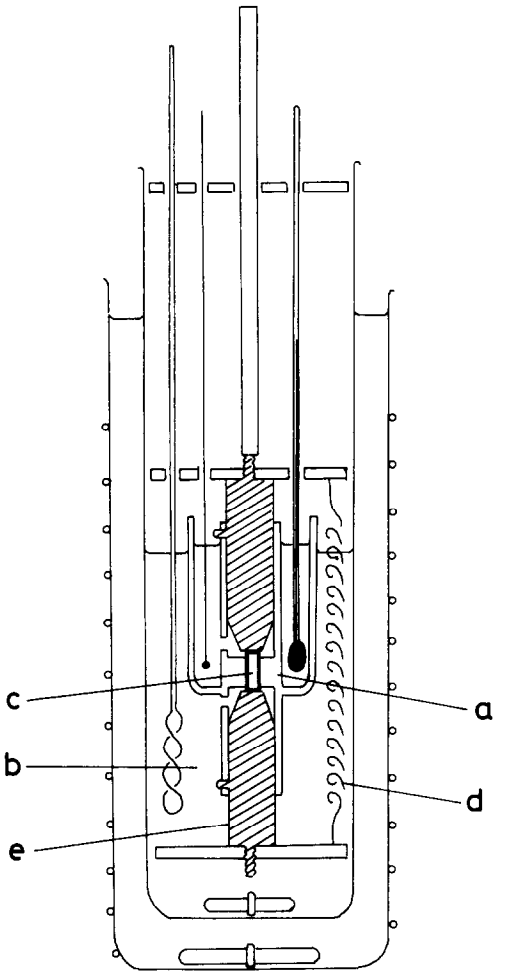

FIG. 5. Section through conductivity jig, (a) glass partition, (b) H_3PO_4 solution, (c) HUP disk, (d) springs, (e) Pd-blacked stainless-steel plungers.

conductivities and activation energies obtained using these two types of electrode systems and the electrodes used earlier.

At close to 274°K both sets of data show a sudden drop-off. This was at first thought to be due to grain-boundary freezing (*10*), but precise measurements of the temperature of the transition have shown it to be between 274 and 275°K, and conclusively above 273°K. A peak in the DTA also occurs at the same temperature and above 273°K (*32*) and has been ascribed to a dielectric transition, occurring some 30°K lower than that reported for the analogous arsenate (*33*). Below the transition temperature complicated frequency dependencies develop (*10*), and a full treatment of the conductivity behavior in the dielectrically ordered phase will be published separately. The conductivity of the arsenate, also to be published shortly, shows a sudden drop-off at about 301°K, the dielectric transition temperature.

Let us return to consider the nature of the disk conductivity. The experiments performed over a range of pH values showed that the conductivity could not be attributable to extrinsic grain-boundary effects, leaving intrinsic grain boundary and bulk conduction to be considered. The sudden and pronounced drop-off in the conductivity at the dielectric transition indicates that bulk conduction accounts for at least most of the conductivity. A small effect from intrinsic grain boundary conduction cannot at this stage be ruled out, and it is possible that the conductivities and activation energies obtained from a single crystal (measurements of which are in progress) may yield slightly different values.

We attribute the bulk conductivity of HUP to proton motion within the water-filled planes of the structure. There are no apparent conduction pathways in the crystal structure which would allow conduction through the uranyl–phosphate layers in a direction perpendicular to the planes. The conductivity value measured parallel to the disk flats was, in the above experiment, three times higher than in the perpendicular direction due to the conduction anisotropy. This factor was found to be typically 3 to 10, depending on the degree of transparency of the disks, and assuming no intrinsic grain-boundary effects, corresponds to an average deviation from a perfect parallel crystallite alignment with the disk flats of 18° and 6° respectively. This is consistent with the X-ray data discussed previously. The expected single-crystal conductivity parallel to the

layers would then be larger than that found parallel to the disk flats by $1/\cos 18° = 1.05$ or $1/\cos 6° = 1.005$.

A third set of results was obtained at higher temperatures for the perpendicular direction using electrodes pressed on during the disk fabrication, as above, but this time using an atmosphere of air and water vapor. The whole conductivity jig was placed in a large vessel containing a small amount of heated water. The jig, situated in the air space, could be independently heated using heater coils wound around it. A temperature controller maintained the jig at 1–5°K above the surrounding gas temperature to prevent water condensation.

Although the results showed a large scatter, the conductivity was shown to be continuous up to 375°K, in this case in a purely steam atmosphere. The values fitted a straight-line extrapolation of the perpendicular data. Dehydration of HUP to a lower water form can thereby be suppressed at 375°K. Indeed NMR measurements (*32*) showed no discontinuity in parameters up to 430°K in a sealed glass tube, and it would be expected that even higher conductivity values could be obtained at this temperature in a pressurized steam atmosphere. The scatter on the data was attributed to loss of wetting of the electrode–HUP interface. This problem proved to be difficult to remedy with this experimental arrangement. In addition there was evidence of electrode polarization at these high current densities.

The range of experiments described above, using different pH values, electrode systems, and frequencies has established the bulk nature of the conduction process and determined that the values of the conductivity and the activation energies obtained are not influenced by electrode or interface effects. That the conductivity is protonic in nature can be deduced from the fact that a steady dc current could be drawn from a H_2–O_2 fuel cell containing HUP as the solid electrolyte. An open cell voltage of 1.0 V was obtained which, after allowing for some nonreversible electrode effects, comes close to the theoretical value of 1.23 V, which would not be inconsistent with a transport number for protons approaching unity, and would certainly indicate a transport number for protons of greater than 0.8. The characteristics of hydride batteries built using HUP support this conclusion (*13*). Anion conduction was shown to be negligible, since a HUP disk could be used to separate two solutions of different pH for extended periods. After immersing disks in HCl solutions, no chloride could be detected in disks using silver nitrate solution, which shows indetectable extrinsic grain boundary uptake.

An upper value for the electronic conductivity in HUP of $10^{-6}\,\text{ohm}^{-1}\,\text{m}^{-1}$ at 295°K was obtained by measuring the dc resistance at 1 V applied potential using ionically blocking indium electrodes.

Discussion

H-Bond Network in HUP

A plan of the HUP structure is shown in Fig. 6a. The UO_2^{2+} ions are perpendicular to the plane and are coordinated in the basal positions to four oxygens from four phosphate groups. The phosphate tetrahedra are twisted with respect to those above and below to produce a two-layer unit cell. The water molecules occupy crystallographically equivalent positions and lie in linked squares which form a continuously H-bonded network, which is illustrated in Fig. 6b. Each water-type oxygen is linked to an oxygen from a phosphate (a *p* bond of average length 283 pm); to an oxygen from an adjacent square by a rather short link bond (*l*) of average length 256 pm, and to two oxygens in the same square (*s* bonds) of average length 281 pm (*29*). For every four water molecules in the formula unit, there are thus 10 O–O pairs capable of forming hydrogen

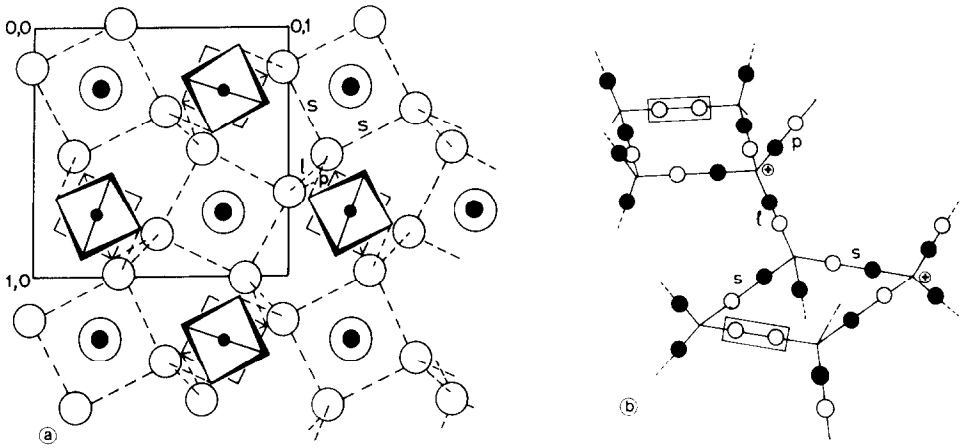

FIG. 6. (a) Projection of the HUP structure along (001). Encircled large black dots, UO_2^{2+}; squares about small dots, PO_4^{3-}; medium open circles, water oxygens. H-Bonds are shown as dashed lines (*29*). (b) H-Bond network in HUP, showing a possible H distribution. The oxygens at the intersections of the lines are not shown. Filled circles, H positions; open circles, unfilled positions. H-Bond vacancies are signified by rectangles.

bonds, but only nine hydrogens available, leaving an empty O–O pair, or H-bond vacancy, to form what might be described as an unsaturated H-bond system.

General Features of Conduction

The ionic conductivity σ of a material is given by the relationship $\sigma = ne\mu$, where n is the number of charge carriers per unit volume and e is the carrier charge. The values obtained or estimated for n and μ for a range of proton conductors are compared in Table I.

In the case of HUP, it is useful to consider the charged species as H_3O^+, the existence of which is supported by ir evidence (*25, 27*). One in four of the equivalent interlamella sites therefore carries a positive charge: three out of four carry no charge and are occupied by water molecules. Conductivity thus occurs by transport of the positive charges among the larger number of otherwise neutral sites. The maximum number of mobile charges equals the number of H_3O^+ ions per unit volume, and this is the figure given in Table I, together with the minimum mobility deduced therefrom. If some of the H_3O^+ ions are essentially trapped then the number of mobile charges will be less than the number of charges present, and the corresponding mobility will be larger. Although the phosphate oxygens could potentially trap

TABLE I

CONDUCTIVITY PARAMETERS OF SOME PROTON CONDUCTORS

	σ (ohm^{-1} m^{-1})	E (kJ mole^{-1})	n (m^{-3})	μ (m^2 V^{-1} sec^{-1})	Ref.
1 *M* HCl (298°K)	40	11	6×10^{26}	4×10^{-7}	(*34*)
HUP (290°K)	0.4	31	$\leq5\times10^{27}$	$\geq5\times10^{-10}$	
$Cu(HCOO)_2\cdot4H_2O$ (270°K)	6×10^{-5}	54	Small		(*11*)
Ice (263°K)	1×10^{-8}	34	$<3\times10^{17}$	5×10^{-7}	(*5, 6*)
KH_2PO_4 (295°K)	6×10^{-10}	73	Small		(*3*)

the excess H^+ in the *p* bonds, as

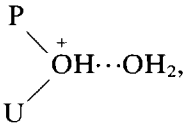

there is no evidence of a P–OH entity in the ir spectrum (*25, 27*) until dehydration has occurred. On the other hand, the presence of H_3O^+ bonds in the ir indicates the

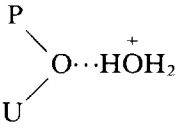

configuration, as would be expected, since the basicity of the phosphate oxygens is greatly reduced by coordination to the U(VI) ion. The proportion of trapped H^+, if any, must therefore be quite small.

Such a generally high concentration of free charge carriers contrasts with those found in the classical proton conductors, as can be seen from Table I. It is this unique feature of HUP which explains its unusually high conductivity. The concentration of charge carriers resembles that in acidic solutions, and the value for a 1 *M* HCl solution is given for comparison in Table I. It would seem likely that a similar explanation also accounts for the high proton conductivities found in $H_3PMo_{12}O_{40}\cdot 30H_2O$ and $H_3PW_{12}O_{40}\cdot 29H_2O$ (*8*). On the other hand, in copper formate tetrahydrate and potassium dihydrogen phosphate, listed in the table, the acidic protons are trapped at basic sites and are inhibited from moving within the H-bond network. In ice the charge carrier concentration is small since self-dissociation into H_3O^+ and OH^- is the only source of intrinsic carriers.

The table also shows the available mobility values. It is clear that the mobility in HUP is unlikely to exceed that found in aqueous solutions or in ice and most likely has a much lower value. Figures for the mobility in ice have shown a downward trend from the early values of $10^{-5}\ m^2\ V^{-1}\ sec^{-1}$ to more recent values near $10^{-7}\ m^2\ V^{-1}\ sec^{-1}$ (*5, 6*) which have been quoted in the table. The present, still somewhat limited, understanding of ice is reviewed by Glasser (*5*) and Franks (*6*). The unusually high conductivity found in HUP is therefore not the result of a high H^+ mobility, but of the abnormally high concentration of free charge carriers.

Intramolecular and Intermolecular Transfer Steps

We turn now to consider the mechanism of conduction in HUP. Continuous proton transport through the H-bond network in HUP requires two types of step: intermolecular H^+ transfer and intramolecular transfer. We shall refer to these as hopping and reorientation, respectively. H^+ transport by each of these processes is illustrated in Figs. 7 and 8. We shall consider each of these processes in turn below.

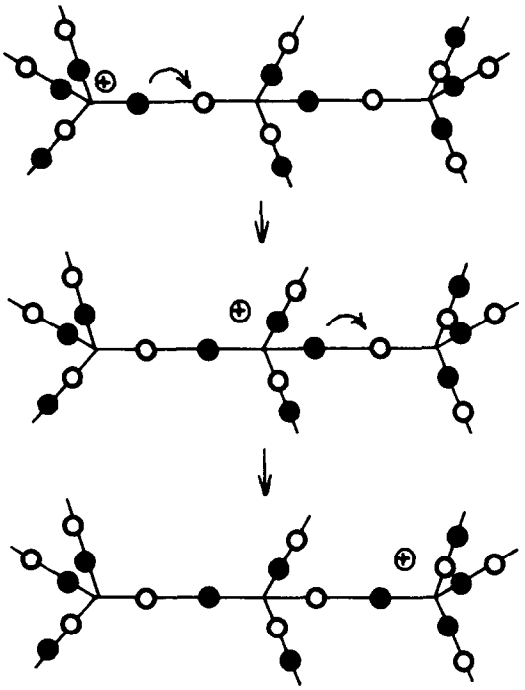

FIG. 7. Sequence of H-hops resulting in motion of charge. Notice how the conduction pathway has become polarized so that a repetition of this sequence could not occur.

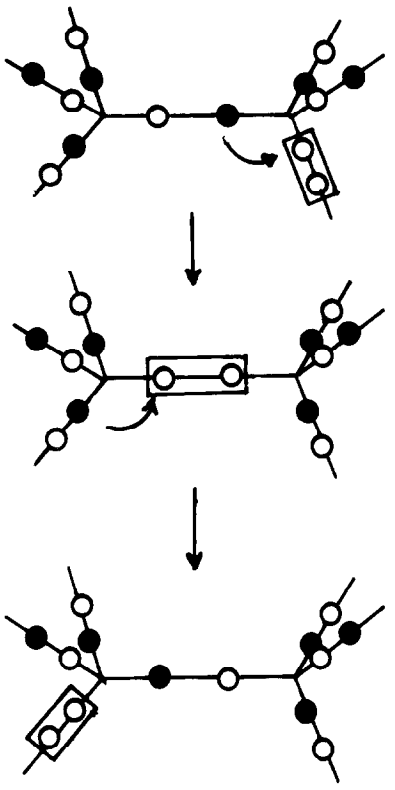

FIG. 8. Motion of charge via intramolecular transfer of H, as shown by the arrows. In the vacancy mechanism, as depicted, vacancies move in the opposite direction to H.

The sequence in Fig. 7 shows intermolecular transfer between H_3O^+–H_2O pairs. Since the initial and final states have the same energies the barrier height will be given by the hopping energy E_h. Some authors have considered this as a tunneling process (*5*). Hopping between pairs of water molecules will be disfavored by the large energy needed to create OH^- and H_3O^+, which is 57 kJ mole^{-1} in water (*6*, p. 504). For the activation energy of hopping in HUP to be less than 10 kJ mole^{-1}, as typically found in H-bonded systems (*5*), the O–O distances need to be close to that of a normal hydrogen bond. The two distances of 256 and 281 pm in HUP (*29*), which are averaged over the occupied and empty bonds, are in fact slightly smaller than the value in ice of 286 pm. The dimensions of the UO_2–PO_4 layers, into which the water molecules pack, thus permit somewhat short H-bond lengths in HUP, even though the bond angles are quite acute.

The second step necessary for continuous conduction, namely, intramolecular transfer, is that by which the molecules reorient to enable continued conduction in a given direction. This can be considered as a resetting of the hydrogens on the side of the O–O vector favorable for conduction. This takes place, in the case of solutions, by the rapid reorientation of water molecules in a continuously fluctuating molecular environment. Hopping in solutions probably then takes place with a very low activation energy when two molecules collide, and indeed the activation energy for H^+ conduction of 11 kJ mole^{-1} (*34*) is close to that for reorientation of approximately 10 kJ mole^{-1} in the vicinity of 295°K (*6*, p. 237).

At the other extreme is the situation where waters of hydration have well-defined sites in a crystalline solid. In this case there are three possible mechanisms for intramolecular transfer. First, a proton may leave a hydrogen bond and enter an adjacent hydrogen bond which already contains a proton, thus forming a Bjerrum D-defect, and leaving behind an L-defect (vacancy), as illustrated diagrammatically:

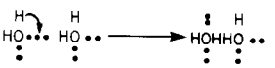

I

The whole molecule may rotate, or one particular proton may just switch bonds, as shown. The formation energy of a D-defect, and an associated L-defect, is 67 kJ mole^{-1} in ice (*6*, p. 143).

The second mechanism is for a proton to leave a hydrogen bond and move into a new bond position which was previously unoc-

cupied, in the following manner

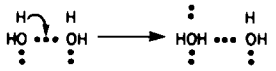

II

The third mechanism is a cooperative motion of two or more protons simultaneously, thus

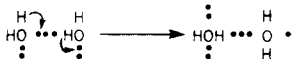

III

However, at the end of the chain a D- or L-defect must nevertheless be involved, unless the chain is circular. The square of four water molecules in HUP affords such an opportunity for cooperative motion.

In the case of HUP, the water molecules will be more restrained in their motion compared to free solution but may retain an enhanced degree of vibrational freedom between the lamellae compared to a normal crystalline solid. Of the three possibilities for intramolecular transfer, **II** the L-defect or vacancy mechanism, is strongly suggested by the high vacancy concentration, although the simultaneous presence of the other two types may also be somewhat favored by the structure (the formation energy of D-defects may be lowered if the two hydrogens formed two bent hydrogen bonds, a situation which is favored by the 90° O–O–O angles within the squares). The utility of the vacancy mechanism would, of course, depend on the vacancies not all being trapped in the water–phosphate (p) positions, which do not form part of the conduction network. However, in the absence of information on this point, the vacancy mechanism must stand as the most attractive one and the results can be satisfactorily explained upon this assumption. Figure 8 shows H^+ motion via vacancy movement, which constitutes resetting of the bonds for further H^+ motion by the hopping step. Vacancy movement could occur by either molecular reorientation, or by one H flipping into the vacancy, as described by von Hippel (*35*), with an activation energy E_{reset}.

Use of the Vacancy Model for the Intramolecular Transfer Step

Assuming the vacancy model, conduction will occur with an activation energy given by $E_{\text{cond}} = E_{\text{h}} + E_{\text{reset}} + E_{C+} + E_{CV} + E_{CV+} + E_{n+} + E_{n\text{V}}$. E_{C+}, E_{CV}, and E_{CV+} are terms arising from the configurational interactions between the defects in their successive configurations, involving H_3O^+–H_3O^+ (E_{C+}), vacancy–vacancy (E_{CV}) and vacancy–H_3O^+ (E_{CV+}) coulombic interactions respectively. E_{n+} and $E_{n\text{V}}$ are terms to take account of any possible trapping of the positive charges onto the phosphate oxygens or of the vacancies into the p bonds, respectively.[2] The activation energy for H-diffusion, as observed in the NMR, contains several different terms, and we have previously related these differences to the different observed activation energies obtained from conductivity and NMR data (*32*). In the present treatment we have added the last three terms in E_{cond} above for completeness, although E_{n+} is not expected to be appreciable, as previously discussed.

So far we have only considered an idealized H-bonded network. When we consider the actual structure found in HUP we find that there will be two basic rates for both hopping and resetting, depending on whether square or link bonds are involved. Conduction necessarily involves the passage of charge through both square and link positions. The link bonds are shorter than the square bonds, which will favor rapid hopping, but may substantially hinder resetting

[2] It might be noted that if the concentration of charge carriers is extremely small, and is exceeded by the number of orientational defects such as L- or D-defects, as in the case of ice just below 273°K, resetting will occur such that there will always be a possible pathway for the charge, and the resetting energy will not appear as a term in the conductivity expression.

involving the link bonds. The difference in bond energies for bonds of 256 and 281 pm can be estimated as approximately 10–20 kJ mole^{-1} (*36*). Thus resetting of the link sites may be a limiting process in the conductivity, with the possibility of more rapid motion of charge in a localized fashion within the squares. In addition to these considerations, the spread of local environments will produce a spread of barrier heights for the hopping and resetting steps.

In conclusion, we find that the high conductivity of HUP can be accounted for on the basis of a high concentration of free charge carriers within a hydrogen-bonded network. The mobility of the charge carriers, although not particularly high, is dependent on a combination of features, and is explained in terms of a coupled hopping–resetting sequence in the presence of possible configurational interactions. We propose that facile reorientation is enabled by the presence of H-bond vacancies in the structure. Both intermolecular hopping and vacancy motion constitute movement of H^+ and therefore constitute conductive steps. However, due to the need for resetting, neither hopping alone, nor vacancy motion alone, can sustain dc conductivity: both are required, on a one-to-one basis, for dc conductivity to occur. Of course both hopping and vacancy motion will be occurring randomly throughout the network, and the conductivity only represents the net flux. The flux due to H^+ hopping will be in the same direction and equal to that due to H^+ motion due to reorientation (or vacancy motion in the opposite direction: compare Figs. 7 and 8). We note that random vacancy motion coupled with random hopping constitutes a mechanism for tracer diffusion. More rapid tracer diffusion may, however, occur by a second mechanism, that of combined random hopping and H_3O^+ reorientations, and NMR relaxation has been explained using this second mechanism (*32*).

Comparison with Solutions and Ice

In a comparison of the mobility of the charge carriers in HUP to those in aqueous solutions on the one hand (*34*), and ice on the other hand (*5, 6*), three features need to be considered: intermolecular transfer (hopping), intramolecular transfer (reorientation), and configurational interactions. In ice just below 273°K the mobility would appear to be determined by hopping, and, since the hydrogen bond network is rigid-like the possibility exists of cooperative hopping (reaction **III**). Only at the lowest temperatures does the resetting achieved by reorientation become significant. Just below 273°K the conductivity, which exhibits an activation energy of 34 kJ mole^{-1}, is not limited by reorientation, which has an activation energy of 58 kJ mole^{-1}.

In acid solution, on the other hand, discrete hopping of one proton may occur upon collision of a suitably oriented water molecule and an H_3O^+ ion, so that the hopping and reorientation steps are coupled as described by the Grotthus mechanism (*34*). The similarity of the activation energies for conduction and reorientation implies that configurational interactions, at least for 1 *M* solutions, are minimal, and that the hopping energy during a collision is very small.

Whereas the mobility in ice is governed by the hopping step, and in acid solutions it is governed by reorientation, in HUP, which retains a Grotthus-type mechanism, both of these factors would appear to be important, and in addition the configurational interaction may be appreciable. Cooperative hopping, although possible, will be less favorable than in ice because of the less rigid H-bonded structure in HUP.

Acknowledgment

One of us, M.G.S., thanks the SRC for a Postdoctoral Fellowship.

References

1. G. ALBERTI, M. CASCIOLA, U. COSTANTINO, G. LEVI, AND G. RICCIARDI, *J. Inorg. Nucl. Chem.* **40**, 533 (1978).
2. R. S. BRADLEY, D. C. MUNRO, AND S. L. ALI, *J. Inorg. Nucl. Chem.* **32**, 2513 (1970).
3. M. SHARON AND A. K. KALIA, *J. Solid State Chem.* **21**, 171 (1977).
4. J. BRUININK, *J. Appl. Electrochem.* **2**, 239 (1972).
5. L. GLASSER, *Chem. Rev.* **75**, 21 (1975).
6. F. FRANKS (Ed.), "Water, a Comprehensive Treatise," Chap. 4, Vol. 1: "The Physics and Physical Chemistry of Water," Plenum, New York (1972).
7. P. GOSAR AND M. PINTAR, *Phys. Status Solidi* **4**, 675 (1964).
8. O. NAKAMURA, T. KODAMA, I. OGINO, AND Y. MIYAKE, Japan Kokai Patent 76106683 (1976).
9. A. T. HOWE AND M. G. SHILTON, U.K. Patent Application 47470 (1976).
10. M. G. SHILTON AND A. T. HOWE, *Mater. Res. Bull.* **12**, 701 (1977).
11. K. E. MURPHY AND T. B. FLANAGAN, *J. Chem. Soc. Faraday II* **73**, 1188 (1977).
12. P. E. CHILDS, M. G. SHILTON, AND A. T. HOWE, unpublished results.
13. P. E. CHILDS, A. T. HOWE, AND M. G. SHILTON, *J. Power Sources* **3**, 105 (1978).
14. A. F. WELLS, "Structural Inorganic Chemistry," 3rd ed., p. 652, Oxford Univ. Press, New York/London (1962).
15. F. WEIGEL AND G. HOFFMANN, *J. Less-Common Metals* **44**, 99 (1976).
16. L. BOURGEOIS, *Bull Soc. Chim. Ind.* **19**, 733 (1897).
17. J. M. SHCHEYER AND C. F. BAES, *J. Amer. Chem. Soc.* **76**, 354 (1953).
18. V. ROSS, *Amer. Mineral* **40**, 917 (1955).
19. A. WEISS, K. HARTL, AND U. HOFFMANN, *Z. Naturforsch. B* **12**, 668 (1957).
20. V. PEKAREK AND M. BENESOVA, *J. Inorg. Nucl. Chem.* **26**, 1743 (1964).
21. V. PEKAREK AND V. VESELY, *J. Inorg. Nucl. Chem.* **27**, 1151 (1965).
22. V. VESELY, V. PEKAREK, AND M. ABBRENT, *J. Inorg. Nucl. Chem.* **27**, 1159 (1965).
23. K. WALENTA, *Chem. Erde* **24**, 254 (1965).
24. G. R. WILLIAMS, *Bol. Inst. Geocienc. Astron. Univ. Sao Paulo* **2**, 83 (1971).
25. I. KH. MOROZ, A. A. VALUEVA, G. A. SIDORENKO, L. G. ZHILTSOVA, AND L. N. KARPOVA, *Geokhimiya USSR* **2**, 210 (1973).
26. L. V. KOBETS, M. V. NIKANOVICH, L. S. GOROSHKO, G. G. NOVITSKII, V. V. SIKORSKII, AND D. S. UMREIKO, *Zh. Neorg. Khim.* **20**, 599 (1975); *Russ. J. Inorg. Chem.* **20**, 334 (1975).
27. M. V. NIKANOVICH, G. G. NOVITSKII, L. V. KOBETS, T. A. KOLEVICH, V. V. SIKORSKII, AND D. S. UMREIKO, *Koord Khim.* **2**, 253 (1976); *Coord. Chem. (Russian)* **2**, 192 (1976).
28. L. V. KOBETS, T. A. KOLEVICH, D. S. UMREIKO, AND V. N. YAGLOV, *Zh. Neorg. Khim.* **22**, 45 (1977); *Russ. J. Inorg. Chem.* **22**, 23 (1977).
29. B. MOROSIN, *Phys. Lett. A* **65**, 53 (1978).
30. M. ROSS AND H. T. EVANS, *Amer. Mineral* **49**, 1578 (1964).
31. M. ROSS, H. T. EVANS, AND D. APPLEMAN, *Amer. Mineral.* **49**, 1603 (1964).
32. P. E. CHILDS, T. K. HALSTEAD, A. T. HOWE, AND M. G. SHILTON, *Mater. Res. Bull.* **13**, 609 (1978).
33. M. A. R. DE BENYACAR AND H. L. DE DUSSEL, *Ferroelectrics* **9**, 241 (1975).
34. J. O'M. BOCKRIS AND A. K. N. REDDY, "Modern Electrochemistry," Vol. 1, Chap. 5, Macdonald Press, London (1970).
35. A. VON HIPPEL, *J. Chem. Phys.* **54**, 145 (1971).
36. H. EYRING (Ed.), "Physical Chemistry," Vol. 5, Chap. 8, Academic Press, New York (1970).